



# VLSI Design of a Processor for Discrete Wavelet Packet and Hilbert Transforms

Peter Yusuf Dibal<sup>1</sup>, Elizabeth N. Onwuka<sup>2</sup>, James Agajo<sup>3</sup>, Caroline O. Alenoghena<sup>2</sup>  
and Achonu Adejo<sup>2</sup>

<sup>1</sup>Computer Engineering Department, University of Maiduguri, Maiduguri, Nigeria

<sup>2</sup>Telecommunications Engineering Department, Federal University of Technology Minna, Minna, Nigeria

<sup>2</sup>Computer Engineering Department, Federal University of Technology Minna, Minna, Nigeria

Received 12 Mar. 2020, Revised 31 Jul. 2020, Accepted 5 Aug. 2020, Published 1 Jan. 2021

**Abstract:** Very Large Scale Integration (VLSI) design is a technological advancement in electronics that has widely shortened the window from concept to a working prototype in any design. It has also made it possible to design and develop sophisticated and intelligent electronic systems which are easily adaptable to any field of human endeavor with relative ease. In this paper, the VLSI design of a processor system is presented, which implements two transforms i.e. the discrete wavelet packet, and the Hilbert transforms. The combination of these two transforms in a single processor makes it possible to have a system with enhanced sub-band frequency edge detection in a wideband signal and other specialized areas, which is very useful in such specialized areas of application as spectrum sensing in cognitive radio networks. The results obtained from the simulation and design verification of the processor system showed the effectiveness of the design methodology presented in this paper. As a matter of fact, the arithmetic operators designed in this paper outperformed the arithmetic operators of the Xilinx IP CORE when compared in terms of speed. From the results obtained, it was clear that the processor design performed as expected, at a great speed.

**Keywords:** Processor, Discrete Wavelet Packet Transform, Hilbert Transforms, FIR Filter, Lifting Steps

## 1. INTRODUCTION

Processor design is important in the electronics world; it makes it possible to design and develop electronic systems and devices, which have practical and viable applications in solving real-life problems. The design approach for processors varies based on the expected functionality of the processor. It could range from simple, medium, to complex processors. Also, depending on the level of complexity of the processor, the associated tools for the design vary in sophistication. Simple and medium range processors usually perform a limited number of tasks, and are thus said to be application-specific, while the complex range processors perform a large number of tasks, which spread across different applications, and are thus said to be non-application-specific. This paper focuses on the design of a processor of the medium range category, which will be used to perform Discrete Wavelet Packet Transform (DWPT) function enhanced with a Hilbert transform (HT). The output of the DWPT stage of the design will be enhanced for better signal representation by passing it

through a Hilbert transform stage. We refer to our work in [1] for exactly how this enhancement is achieved mathematically.

To realize the objective of this paper, two design approach will be used. The first design approach is the lifting step, which will be used in the processor-design-implementation of the DWPT transform. The second design approach is the Finite Impulse Response (FIR) filter design, which will be used to perform the processor-design-implementation of the Hilbert transform. As stated earlier, the tools employed in the design of processors vary in sophistication and level of complexity. For the design in this paper, the tool of choice is the VHSIC (Very High Speed Integrated Circuit) Hardware Description Language (VHDL). VHDL is a powerful, independent, portable, and reusable language, which is used in the design of medium to complex range processors [2]. It allows the description of the behavior of an electronic device from which the physical circuit can be realized. Further information on VHDL can be found in [3]–[5]. Once the circuit is realized, it can then be implemented on a Complex



Programmable Logic Device (CPLD) or Field Programmable Gate Array (FPGA). In this paper, the target device is an FPGA.

#### A. Review of Related Works in Wavelet Processor Design

Quite a number of research has been done in the development of processors for wavelet transforms; the authors in [6] proposed a wavelet processor based on the lifting scheme that had no multipliers but with reduced complexity, it however has low efficiency in area requirements. An efficient dual mode Integer Haar Lifting Wavelet Transform (IHLWT) was proposed in [7], which had reduced requirements by exploiting arithmetic operations redundancies involved with IHLWT computations; the architecture was also multiplier-free and performed IHLWT with a single adder and subtractor. In [8], the authors proposed a DWT architecture based on word serial pipeline and parallel filter processing in which high and low-pass filters were used concurrently at each level; this approach made the design work twice faster than most traditional designs. Using residue number system, the authors in [9] proposed the design of a 2-dimensional DWT processor. A symmetric extension scheme was employed by the design to reduce distortion at image boundaries.

#### B. Review of Related Works in Hilbert Transform Processor Design

In the design of Hilbert transform processors, authors have used different approaches to realize their objectives. As an example, the authors in [9] proposed a low power and fast reconfigurable Hilbert transform processor based on ripple carry adder and carry save adder thereby bypassing multipliers; power reduction was achieved by turning off adders when the multiplier operands were zero. Using fast Fourier transform (FFT), the authors in [10] designed a HT processor by multiplication with  $+j$  and  $-j$  in the frequency domain; an efficient signal flow graph was developed in the design by utilizing decimation-in-frequency and decimation-in-time approach. For approximations in image applications based on HT, the authors in [11] proposed a model that exploited the symmetry and alternating zero-valued coefficients of an HT-FIR filter in the generation of in-phase and quadrature components that were essential for envelope computation. The target FPGA for their design was the Stratix IV FPGA on a Terasic DE4-230 board. The authors implemented a hardware for computing the instantaneous frequency of a phonocardiogram using discrete HT. Their design involved the use of a system level modeling tool for DSP, a System Generator provided by Xilinx in Simulink to achieve a faster design cycle. The results obtained from their design were similar to those computed using MATLAB.

The rest of this paper is organized as follows: we review in section 2, the DWPT and the mechanism by which it decomposes a signal alongside an analysis of the DWPT lifting steps. Section 3 presents the implementation of the floating point arithmetic operations that will be used in the lifting steps; the implementation involves the use of logic gates and buffers. In section 4, the Hilbert transform is presented with its design using FIR filter technique; in section 5, a complex finite-state-machine (CFSM) design of the wavelet processor stage is shown; the design in this section is based on the lifting steps in section 2. Section 6 presents the design of the Hilbert transformer stage of the processor; this section builds on section 4 and also utilizes a CFSM in the design, while section 7 presents the simulation of the designs made, the verification of the designs, and also performance measurement. Finally, a conclusion is presented in section 8.

## 2. DISCRETE WAVELET PACKET TRANSFORM (DWPT)

In signal processing, DWPT belongs to the category of wavelet transforms. It operates by representing known and unknown signal features through wavelet basis. DWPT can be viewed as a generalization of the wavelet transform, and it uses filter banks arranged in a tree structure format when implementing a wavelet algorithm. A typical example of a DWPT tree is shown in Fig. 1[12], where the decomposition of a signal is implemented by a low-pass (H) and high-pass filter (G) pairs i.e. H-G pairs. Each parent node decomposing an input signal in Fig. 1 is split into two subspaces  $W_{n,j}$  which has the property of orthogonality, and is mathematically expressed as:

$$W_{n,j} = W_{2n,j-1} \oplus W_{2n+1,j-1} \quad (1)$$

where  $n$  is a nonnegative integer,  $j$  is the decomposition level, and  $\oplus$  is orthogonal addition. The wavelet packet coefficients  $\xi_{l+1}^{2p}[n]$  are generated using the scaling filter, and the coefficients  $\xi_{l+1}^{2p+1}[n]$  are generated using the wavelet filter. The coefficients are mathematically expressed as [12]:

$$\xi_{l+1}^{2p}[n] = \sqrt{2} \sum_k h[k] \xi_l^p[2n-k], n = 0, 1, \dots, N-1 \quad (2)$$

$$\xi_{l+1}^{2p+1}[n] = \sqrt{2} \sum_k g[k] \xi_l^p[2n-k], n = 0, 1, 2, \dots, N-1 \quad (3)$$

where  $h[k]$  is the low-pass filter,  $g[k]$  is the high-pass filter, and  $p$  is the position at level  $l$ . For the signal in each subband channel, the energy is calculated as [13]–[15]:

$$E = \frac{1}{T} \int_0^T \left[ \sum_{j \geq j_0} \sum_k c_{j,k} \phi_{j,k}(t) + d_{j,k} \psi_{j,k} \right]^2 dt \quad (4)$$

$$E = \frac{1}{T} \sum_{j \geq j_0} \sum_k (c_{j,k}^2 + d_{j,k}^2) \quad (5)$$

where  $c_{j,k}$  is scaling function coefficient,  $d_{j,k}$  is the wavelet function coefficient.

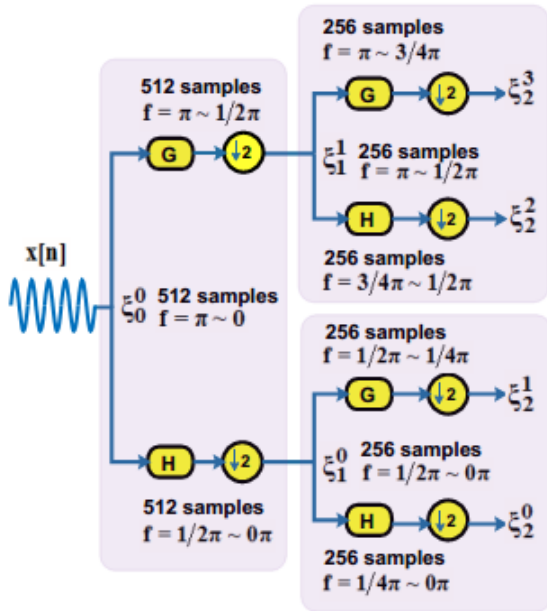


Figure 1. Analysis filter bank of a wavelet packet

According to [16], the decomposition functions in (2) and (3) can be factored into lifting steps for an orthogonal Daubechies wavelet with 4 vanishing moments (Db4) as shown below in (6):

$$\left. \begin{aligned} s_{j+1}^{(1)}[n] &= s_j[2n] + \sqrt{3}s_j[2n+1] \\ d_{j+1}^{(1)}[n] &= s_j[2n+1] - \frac{1}{4}\sqrt{3}s_{j+1}^{(1)}[n] - \frac{1}{4}(\sqrt{3}-2)s_{j+1}^{(1)}[n-1] \\ s_{j+1}^{(2)}[n] &= s_{j+1}^{(1)}[n] - d_{j+1}^{(1)}[n+1] \\ s_{j+1}[n] &= \frac{\sqrt{3}-1}{\sqrt{2}}s_{j+1}^{(2)}[n] \\ d_{j+1}[n] &= \frac{\sqrt{3}+1}{\sqrt{2}}d_{j+1}^{(1)}[n] \end{aligned} \right\} (6)$$

where  $s_{j+1}[n]$  is the updated value at the next iteration ( $H$  filter output of Fig. 1), and  $d_{j+1}[n]$  is the predicted value at the next iteration ( $G$  filter output in Fig. 1). The lifting steps in (6) is the basis by which the DWPT stage of the processor will be designed, and its close inspection reveals that the incoming signal  $s_j[n]$  is composed of several data points upon which the lifting steps act to achieve discrete wavelet packet transformation of the incoming signal.

For the design in this paper, each of these data points will be represented using the IEEE-754 single precision floating point representation. The IEEE-754 single precision floating point representation of numbers is a 32-bit format representation, consisting of 1-bit sign representation, 8-bit exponent representation, and 23-bit mantissa representation. The structure of the IEEE-754 single precision floating point format is shown in Fig. 2[17].

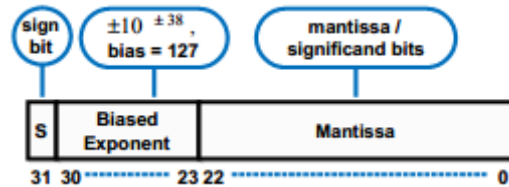


Figure 2. IEEE-754 floating point single precision data format

As an example of this data format, we present in Table 1, the IEEE-754 single precision floating point representation for three samples of an input data.

TABLE I. IEEE-754 SINGLE PRECISION FLOATING POINT DATA REPRESENTATION

S/N	Input Data	IEEE-754 single precision floating point representation
1	0.5377	00111111000010011010011010110101
2	1.8339	00111111111010101011110100111100
3	-2.2588	11000000000100001001000000101110

### A. Analysis of DWPT Lifting Steps

A close inspection of (6) reveals that there are three fundamental arithmetic operations involved in the realization of the lifting steps. These are: multiplication, addition, and subtraction. Owing to the IEEE-754 single precision floating point representation of the data points in  $s_j[n]$ , the arithmetic operations will be floating point in nature; thus the multiplication operation will be IEEE-754 single precision floating point multiplication, the addition will be IEEE-754 single precision floating point addition, and the subtraction will be IEEE-754 single precision floating point subtraction.

To perform floating point multiplication on a pair of 32-bit numbers A and B using the structure shown in Fig. 2, different operations are performed on the constituent parts of the numbers i.e. sign bit, exponent bits, and mantissa bits [18], [19]. We propose the algorithm to achieve this multiplication in Algorithm 1, where s1, e1, and m1 are the sign bit, exponential bits, and mantissa bits of the first number A, and s2, e2, and m2 are the sign bit, exponential bits, and mantissa bits of the second number B.

**Algorithm 1: IEEE-754 Floating Point Unit Multiplier Algorithm**

1	Initialize s1, e1, m1, s2, e2, m2, overflow
2	XOR [ s1, s2 ] → product_sign_bit
3	Add [ e2, (e1 - 127) ] → product_exponent
4	Append [ 1, m1 ] → intermediate_m1
5	Append [ 1, m2 ] → intermediate_m2
6	Multiply [ intermediate_m1, intermediate_m2 ] → product_mantissa
7	If product_exponent > 255
8	1   Assert overflow
9	2   Product_sign_bit → final_sign_bit
10	3   Assert final_product(30 down to 0)
11	4   Append [ final_sign_bit, final_product(30 down to 0) ] → final_product(31 down to 0)
12	End
13	If product_mantissa(47) == 1
14	1   product_mantissa(46 downto 24) → normalized_mantissa
15	2   Add [ 1, product_exponent ] → final_exponent
16	3   Append [ product_sign_bit, final_exponent, normalized_mantissa ] → final_product(31 down to 0)
17	Else
18	1   Product_mantissa( 45 downto 23 ) → normalized_mantissa
19	2   Append [ product_sign_bit, product_exponent, normalized_mantissa ] → final_product(31 down to 0)
20	End

For floating point addition and subtraction, operations will also be performed on the sign bit, exponential bits, and mantissa bits of both numbers A and B [19], [20].

We propose the algorithm shown in Algorithm 2 which is used to achieve floating point addition and subtraction.

**Algorithm 2: IEEE754 - Floating Point Unit Addition and Subtraction Algorithm**

1	Initialize s1, e1, m1, s2, e2, m2	31	Begin: mantissaProcess
2	If e1 == e2	32	If xor ( s1, s2 ) == 0
3	1   Jump to mantissaProcess	33	1   Add ( m1, m2 ) → Result_mantissa
4	End	34	2   OR ( s1, s2 ) → Result_sign
5	If e1 > e2	35	Else if ( m1 >= m2 )
6	1   Sub ( e1, e2 ) → exp_diff	36	1   Sub ( m1, m2 ) → Result_mantissa
7	2   If exp_diff > 23	37	2   s1 → Result_sign
8	1   Result_mantissa → m1	38	Else if ( m1 < m2 )
9	2   Result_sign → s1	39	1   Sub ( m2, m1 ) → Result_mantissa
10	3   Result_exponent → e1	40	2   s2 → Result_sign
11	4   Jump to exitProcess	41	End if
12	3   Else	42	End: mantissaProcess
13	1   m2 ( 24 downto exp_diff ) → m2	43	If ( Result_mantissa == 0 )
14	2   0 → m2 ( 24: sub ( 25, exp_diff ) )	44	1   0 → Result_mantissa
15	3   Jump to mantissaProcess	45	2   0 → Result_exponent
16	4   End if	46	3   Jump to exitProcess
17	End if	47	Else if ( Result_mantissa(24) == 1 )
18	If e2 > e1	48	1   Append ( 0, Result_mantissa(24:1) ) → Result_mantissa
19	1   Sub ( e2, e1 ) → exp_diff	49	2   Add ( exponent, 1 )
20	2   If exp_diff > 23	50	3   Jump to exitProcess
21	1   Result_mantissa → m2	51	Else if ( Result_mantissa(23) == 0 )
22	2   Result_sign → s2	52	1   Begin loop for j from 0 to 22
23	3   Result_exponent → e2	53	1   If Result_mantissa(j) == 1
24	4   Jump to exitProcess	54	1   Result_mantissa(j+1:0) →
25	3   Else	55	Result_mantissa(24: sub(23, j)
26	1   m1 ( 24 downto exp_diff ) → m1	56	2   0 → Result_mantissa(22-i: 0)
27	2   0 → m2 ( 24: sub ( 25, exp_diff ) )	57	3   (Result_exponent - 23) + j →
28	3   Jump to mantissaProcess	58	Result_exponent
29	4   End if	59	2   End if
30	End if	60	2   End loop
		61	End if
		62	Begin: exitProcess
		63	1   Result_sign → final_result(31)
		64	2   Result_exponent → final_result(30:23)
		65	3   Result_mantissa(22:0) → final_result (22:0)
		66	End: exitProcess
		67	



### 3. IMPLEMENTATION OF LIFTING STEPS USING FLOATING POINT ARITHMETIC

The lifting steps in (6), consists of three fundamental arithmetic operations which are multiplication, addition, and subtraction. All these operations are floating point in nature due to the data representation of the incoming signal. To design the architecture of the processor based on this lifting steps, it is important to analyze the lifting steps in details, and this done as follows:

- The first line in the lifting steps involves splitting the incoming signal values into even and odd components based on their index values. Each odd-indexed signal values are then multiplied by the square root of 3 and then added to the even values to get the first preliminary “update” value of the lifting step.
- In the second line of the lifting steps, we multiply the updated values in (i) above by a factor of  $\sqrt{3}/4$  and subtract the product from the odd-indexed signal values in the original signal. We also multiply the unit delayed values of the updated values in (i) above by a factor of  $(\sqrt{3}-2)/4$  and then subtract the product from the odd-indexed signal values in the original signal. The final result is the first preliminary “predict” value of the lifting step.
- In the third line of the lifting step, we compute the difference between the first preliminary updated values and the first preliminary predicted values to obtain the second preliminary updated values.
- The fourth line of the lifting step involves the multiplication of the second preliminary “update”

values by a factor of  $(\sqrt{3}-1)/\sqrt{2}$  to obtain the final “update” values for the current level of iteration.

- In the fifth line of the lifting scheme, the first preliminary “predict” value is multiplied by a factor of  $(\sqrt{3}+1)/\sqrt{2}$  to obtain the final “predict” values for the current level of iteration.

To efficiently implement the lifting steps using floating point arithmetic based on the analysis above, it is imperative to split all the operations in (6) into what we call distinct atomic operations, and associate each atomic operation with an atomic instruction. Each atomic instruction would thus cause a specific atomic operation to be executed by the processor, and then the wavelet transform of the input signal will be computed by gluing the atomic operations together at different levels during the progressive computation of the transform as defined in the relationship in (6).

From the foregoing therefore, the following atomic instructions are proposed as shown in Table 2, alongside the arithmetic operations they perform. Table 2 actually shows the relationship between the control unit and the data path of the processor to be designed. The atomic instructions will be handled by the control unit of the processor while the atomic operations will be handled by the datapath of the processor. Each of the atomic instructions actually represents a control signal issued from the control unit of the processor, and for each atomic instruction, there will be a corresponding status signal from the datapath which will tell the control unit that a particular operation has been executed. The control unit will then issue the next atomic instruction for the next atomic operation to be executed. This will continue till the control unit issues all the atomic instructions.

TABLE II. ATOMIC INSTRUCTIONS WITH CORRESPONDING ATOMIC OPERATIONS

SN	Atomic Instruction	Atomic Operation	SN	Atomic Instruction	Atomic Operation
1	Ld_reg_2n	$x_{2n\_reg} \leftarrow x\_input(2n)$	8	Ld_diff_one	$diff\_one\_reg \leftarrow x_{2np1\_reg} - rt_{3b4\_sjp1\_1\_reg}$
2	Ld_reg_2np1	$x_{2np1\_reg} \leftarrow x\_input(2n+1)$	9	Ld_djp1_1	$djp1\_1\_reg \leftarrow diff\_one\_reg - rt_{3m2b4\_sjp1\_1\_lsh\_reg}$
3	Ld_reg_rt3_2np1	$rt_{3\_2np1\_reg} \leftarrow (\sqrt{3}) \times x_{2np1\_reg}$	10	Rsh_djp1_1	$djp1\_1\_rsh\_reg(n) \leftarrow djp1\_1\_reg(n+1)$ $djp1\_1\_rsh\_reg \leftarrow 0 \& djp1\_1\_rsh\_reg$
4	Ld_reg_sjp1_1	$sjp1\_1\_reg \leftarrow x_{2n\_reg} + rt_{3\_2np1\_reg}$	11	Ld_sjp1_2	$sjp1\_2\_reg \leftarrow sjp1\_1\_reg + djp1\_1\_rsh\_reg$
5	Ld_reg_rt3b4_sjp1_1	$rt_{3b4\_sjp1\_1\_reg} \leftarrow (\sqrt{3}/4) \times sjp1\_1\_reg$	12	Ld_update	$update\_reg \leftarrow [(\sqrt{3}-1)/\sqrt{2}] \times sjp1\_2\_reg$
6	Lsh_sjp1_1	$sjp1\_1\_lsh\_reg(n) \leftarrow sjp1\_1\_reg(n-1)$ $sjp1\_1\_lsh\_reg \leftarrow sjp1\_1\_lsh\_reg \& 0$	13	Ld_predict	$predict\_reg \leftarrow [(\sqrt{3}+1)/\sqrt{2}] \times djp1\_1\_reg$

7	Ld_rt3m2b4_sjp1_1_lsh	rt3m2b4_sjp1_1_lsh_reg ← $\left[ \frac{(\sqrt{3}-2)}{4} \right] \times$ sjp1_1_lsh_reg	
---	-----------------------	---	--

From Table 2, there will be 13 atomic instructions or control signals, and for each of these, there will be 13 status signals indicating the completion of an atomic operation by the datapath. With such a large number of information-exchange between the control unit and the datapath, it is clear an RT (register transfer)-level approach will not be powerful in designing the processor. The reason is because an RT-level design requires the direct connection of standard components like memories, registers, and counters to obtain desired system functionality; this approach is ideal for small designs characterized by standard functionalities. The design in this paper is a custom design and has non-standard functionality; hence it is imperative to use a complex finite state machine (CFSM). The design of the processor using CFSM will be discussed in Section 6 after an analysis of the design of the Hilbert transformer in Section 4.

#### 4. HILBERT TRANSFORM

The Hilbert transform in signal analysis is a technique that is applied in diverse fields of engineering and science including diagnosis and detection of faults in gear boxes, communication systems, and QRS-wave detection in biomedical engineering [21]–[23]. Hilbert transform has a major advantage over other transforms in the sense that it does not require a change of domain for its operation [24].

Given a real valued signal  $x(t)$ , the Hilbert transform of such a signal is defined as the convolution of  $x(t)$  with  $1/\pi t$ . The parameter  $1/\pi t$  is defined as the kernel of the Hilbert transformer. Mathematically, the Hilbert transform of  $x(t)$  can be expressed as [24]:

$$y(t) = h(t) * x(t) = \frac{1}{\pi t} x(t) \quad (7)$$

$$y(t) = \frac{1}{\pi} \int_{-\infty}^{\infty} x(\tau) \frac{1}{t-\tau} d\tau = -\frac{1}{\pi} \int_{-\infty}^{\infty} x(\tau) \frac{1}{\tau-t} d\tau \quad (8)$$

where  $h(t)$  is the Hilbert transformer. The coupling at  $t = \tau$  is possible owing to the Cauchy principal value of the integral. The summation of  $x(t)$  and its Hilbert transform forms an analytic signal, which is expressed as:

$$z(t) = x(t) + iy(t) \quad (9)$$

For the Hilbert transform of  $x(t)$  in (8) to be implemented on an FPGA, it will have to be expressed in terms of a Finite Impulse Response (FIR) filter. The exact means by which this is achieved is discussed in the following subsection.

##### A. Finite Impulse Response Filter Design of a Hilbert Transformer

Hilbert transforms can be designed using Finite Impulse Response (FIR) filters or Infinite Impulse Response (IIR) filters. However, the FIR filter approach is preferred over IIR filter because it guarantees that the stability and phase response of the filter are less sensitive to effects of rounding coefficients [25].

To design the FIR Hilbert transformer, consider the conceptual representation of the expression in (9) in Fig. 3 with the real output as  $x_r(t)$  and imaginary output as  $y_i(t)$ .



Figure 3. Conceptual Hilbert Transformer

In Fig. 3,  $y_i(t)$  is the convolution of  $x_r(t)$  and  $h(t)$ . This is mathematically expressed as [26]:

$$y_i(n) = \sum_{k=-\infty}^{\infty} h(k)x_r(n-k) \quad (10)$$

The expression in (10) makes it possible to implement a Hilbert transformer as a discrete non-recursive FIR filter according to the structure shown in Fig. 4 [26] where  $x_r(n)$  is the input signal,  $y_i(n)$  the output signal, and  $h(n)$  the coefficients of the filter.

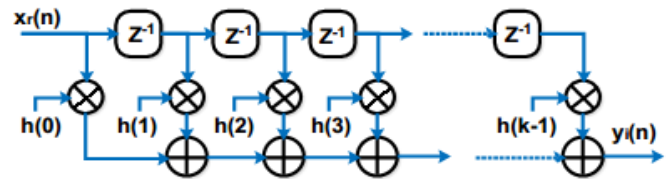


Figure 4. FIR implementation of a k-tap Hilbert Transformer

To design the Hilbert FIR transformer according to the structure shown in Fig. 4, we will utilize the FIR technique having anti-symmetric coefficients with an even number of taps (type III system) [27]. The reason is because even-tap FIR Hilbert transformer is computationally efficient, has low complexity and latency. It should be noted that for the type III Hilbert transformer structure shown in Fig. 4, the  $h(k)$  coefficients have alternate zeros.



For an ideal lowpass filter with cut-off frequency  $w_c = 2\pi f_c / f_s$ , the impulse response is [28]:

$$b(n) = \sin(w_c n) / \pi n, -\infty < n < \infty \quad (11)$$

The expression in (11) is not realizable in hardware owing to the fact that  $b(n)$  spans  $-\infty$  to  $\infty$ . To make it hardware-realizable, we must truncate  $b(n)$  in such a manner that it will give an acceptable approximation of the impulse response. To achieve this, we will truncate  $b(n)$  to  $N+1$  samples and then apply a window technique. Using a halfband filter approach [27], we define  $w_c$  as:

$$w_c = 2\pi/4 = \pi/2 \quad (12)$$

Substituting (12) into (11) yields:

$$b(n) = \sin(n\pi/2) / n\pi, -N/2 < n < N/2$$

Applying a window function  $w(n)$  having a length of  $N+1$ , we obtain the filter coefficients for  $h(n)$  in Fig. 4 as:

$$h(n) = b(n)w(n), -N/2 < n < N/2 \quad (13)$$

$$h(n) = \frac{\sin(n\pi/2)}{n\pi} w(n), -N/2 < n < N/2 \quad (14)$$

The window function  $w(n)$  could be Rectangular window, Barlett window, Hanning window, Hamming window, or Blackman window etc. [29], [30]. In this paper, the choice of our window will be Blackman window because it has a cosine term which reduces side lobes in a signal being processed [31]. This ensures less power wastage and increased efficiency. The Blackman window [29] is presented in (15).

$$w(n) = \begin{cases} 0.42 - 0.5\cos\left(\frac{2\pi n}{N-1}\right) + 0.08\cos\left(\frac{4\pi n}{N-1}\right), & 0 \leq n \leq M-1 \\ 0, & \text{otherwise} \end{cases} \quad (15)$$

TABLE III. FIR HILBERT TRANSFORMER COEFFICIENTS

### 5. WAVELET PROCESSOR STAGE DESIGN USING COMPLEX FINITE STATE MACHINE (CFSM)

In the design of both the wavelet processor stage and the FIR Hilbert transform stage, a CFSM will be used because of the large number of control and potential status signals involved in the design as shown in Table 2. Using either a Moore or Mealy FSM for the entire design becomes impractical because of the presence of circuit components like memory and shift operators. Hence, the use of CFSM is inevitable.

In a processor design, a CFSM is a design approach in which the control unit is designed as an FSM, while the

where  $M = N/2$  for  $N$  even and  $(N+1)/2$  for  $N$  odd.

Exploiting the coefficient symmetry of the FIR filter [32], the FIR filter is designed as shown in Fig. 5a with negative symmetry and an even number of taps [32]. For the FIR filter structure shown in Fig. 5a to perform Hilbert transformation of  $x_r(n)$ , the  $h(k)$  coefficients must have alternating zeros. Hence, the FIR filter structure is redesigned as shown in Fig. 5b, where the alternating zeros can be seen in the coefficients. The impulse response of the FIR Hilbert transform is also shown in Fig. 6a [32].

Using the relationship in (14) and (15), we compute values for  $h(0)$  to  $h(6)$ . These values are shown in Table 3. Fig. 6b shows the impulse response of the FIR Hilbert transformer designed in this paper based on the computed coefficients in Table 3. The reader is referred to [32] for the analysis of signals in an FIR filter.

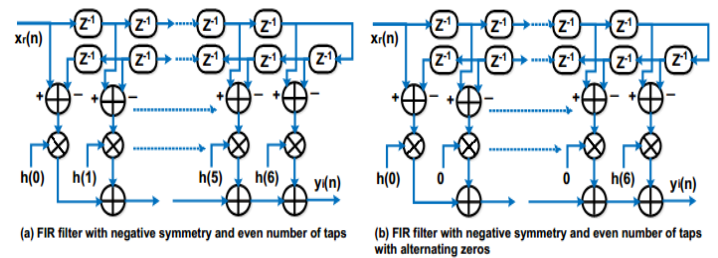


Figure 5. FIR filter coefficient symmetry – even number of taps

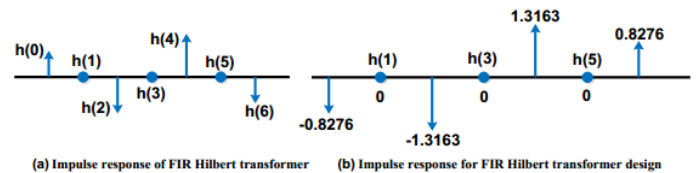


Figure 6. Impulse response of Hilbert transformer based on FIR filter

S/N	1	2	3	4	5	6	7
Filter Coefficients	$h(0)$	$h(1)$	$h(2)$	$h(3)$	$h(4)$	$h(5)$	$h(6)$
Values	-0.8276	0	-1.3163	0	1.3163	0	0.8276

datapath is designed as an RT-level circuit [33]. The control unit design and the datapath design are then integrated together to implement complex processor behavior and functionalities. Table 4 shows the differences between the control unit and the datapath in the context of CFSM [33].



TABLE IV. CFSM-CONTEXT BASED DIFFERENCES BETWEEN CONTROL UNIT AND DATA PATH

S/N	Control unit	Datapath
1	Modeled using FSM	Modeled using RT-level models
2	Defines clock-based sequencing of actions in	Defines synchronous and asynchronous transformation of

The control unit operates on the basis of the values of the present state of the processor which includes the control inputs, and the incoming conditioning signals from the datapath. In each state, the control unit determines the next state to branch to, and the set of control signals necessary to enable the next set of concurrent operations to be performed by the datapath on the next rising edge of the clock.

The datapath is essentially an interconnection of system resources as shown in Table 5, and the execution of operations in the datapath is enabled by the control signals from the control unit. The status signals from the datapath, gives the control unit the precise information to make the appropriate transition through states.

TABLE V. DATAPATH SYSTEM RESOURCE CATEGORIZATION

S/N	Resource category	Resource type
1	Functional resources	Adders, multipliers,
2	Memory resources	Registers, RAM, ROM, D-flip
3	Interface resources	Bus, steering logic, I/O pad

For proper coordination between the control unit and the datapath, synchronization is very important and this is achieved using clock signals. A good synchronization between the control unit and the datapath eliminates the negative effects of timing skew which causes unpredictability in output. Based on the atomic instructions and the atomic operations in Table 2, we propose the design of the wavelet processor stage as shown in Fig. 7 where the interconnection between the datapath and the control based on the atomic instructions and atomic operations of Table 2 can be seen.

## 6. HILBERT TRANSFORM PROCESSOR STAGE DESIGN USING CFSM

Similar to the design of the wavelet stage of the processor, the Hilbert transform stage is also designed using CFSM, where the control unit is implemented using FSM, and the datapath is implemented using RT-level circuit. The complete design is shown in Fig. 8; the design is such that the output from the wavelet processor state is stored in a 16x32 bit RAM called hRAM. At each rising edge of the clock, the contents of hRAM are transferred one-by-one to a 1x32 bit register sequentially. Thus when the control unit is in state S0, the first content of hRAM is transferred to the first 1x32 bit register; when the control unit transits to state S1, the content of the first 1x32 register is transferred to the second 1x32 bit register and so on.

The transfer in this order is possible because unlike the load signal of a current state in the wavelet processor stage which is turned OFF when the control unit makes a transition to the next state, the load signal of the current in the Hilbert transform control unit is not turned OFF when there is a transition to the next state; this makes the register load the next data into the register associated with the previous state, while the current state loads the previous data coming from the previous state.

By this mechanism, the Hilbert transform is able to perform data transfer according to the structure shown in Fig. 5b. As the data is transferred from one 1x32 bit register to the next 1x32 bit register, the necessary computations are performed by the floating point subtractors, multipliers, and adders. When the Hilbert transform stage of the processor completes the computation, it triggers the `ld_reg2n_2np1` signal in the wavelet processor stage which begins another round of computation for another data set.

## 7. DESIGN SIMULATION, VERIFICATION, AND PERFORMANCE MEASUREMENT

In this section, the simulation of the design will be performed, alongside verification of the design. This section will also present the performance of the design starting with the floating point multiplier, adder/subtractor, the wavelet transform stage of the processor, and then the Hilbert transform stage.

Table 6 shows the performance of the floating point multiplier designed using Algorithm 1 where it can be seen that the same level of performance was obtained when compared with the Xilinx IPCORE. The root mean squared error (RMSE) between the Xilinx IPCORE and the proposed multiplier computed using the

relationship[34]  $RMSE = \sqrt{(1/n) \sum_{i=1}^n (x - \hat{x})^2}$  was 0;

where  $n$  is the number of samples,  $x$  the value obtained from Xilinx IPCORE, and  $\hat{x}$  the value from the proposed multiplier. However, the proposed multiplier in this paper was faster in the computation of the product of its input at 650ns as shown in Fig. 9 than that of Xilinx IPCORE at 850ns. Similarly, the floating point adder/subtractor designed using Algorithm 2 gave the same level of accuracy in comparison with the Xilinx IPCORE with an RMSE = 0.00000xxx as shown in Table 7. This value xxx of RMSE i.e. quantization error caused by the difference in the internal representation of floating point numbers between the proposed algorithm and Xilinx IPCORE is insignificant to cause any distortion in computation because it is highly accurate and competes better than similar algorithms[34]–[37]. Fig. 10 shows that the proposed adder/subtractor gave the same level of performance at a lesser time 450ns than the Xilinx IPCORE adder/subtractor time of 1150ns.



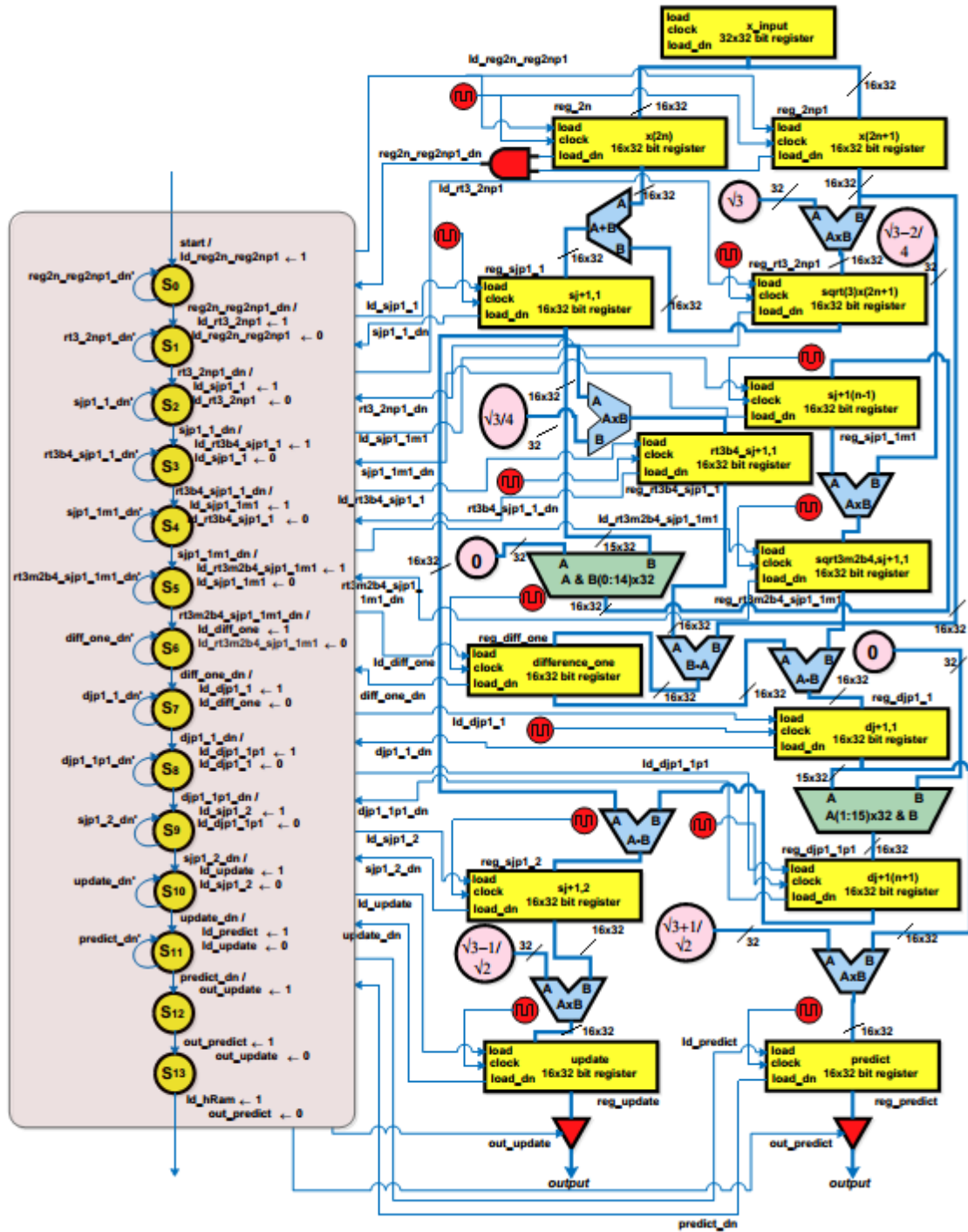


Figure 7. Wavelet processor stage design using CFSM

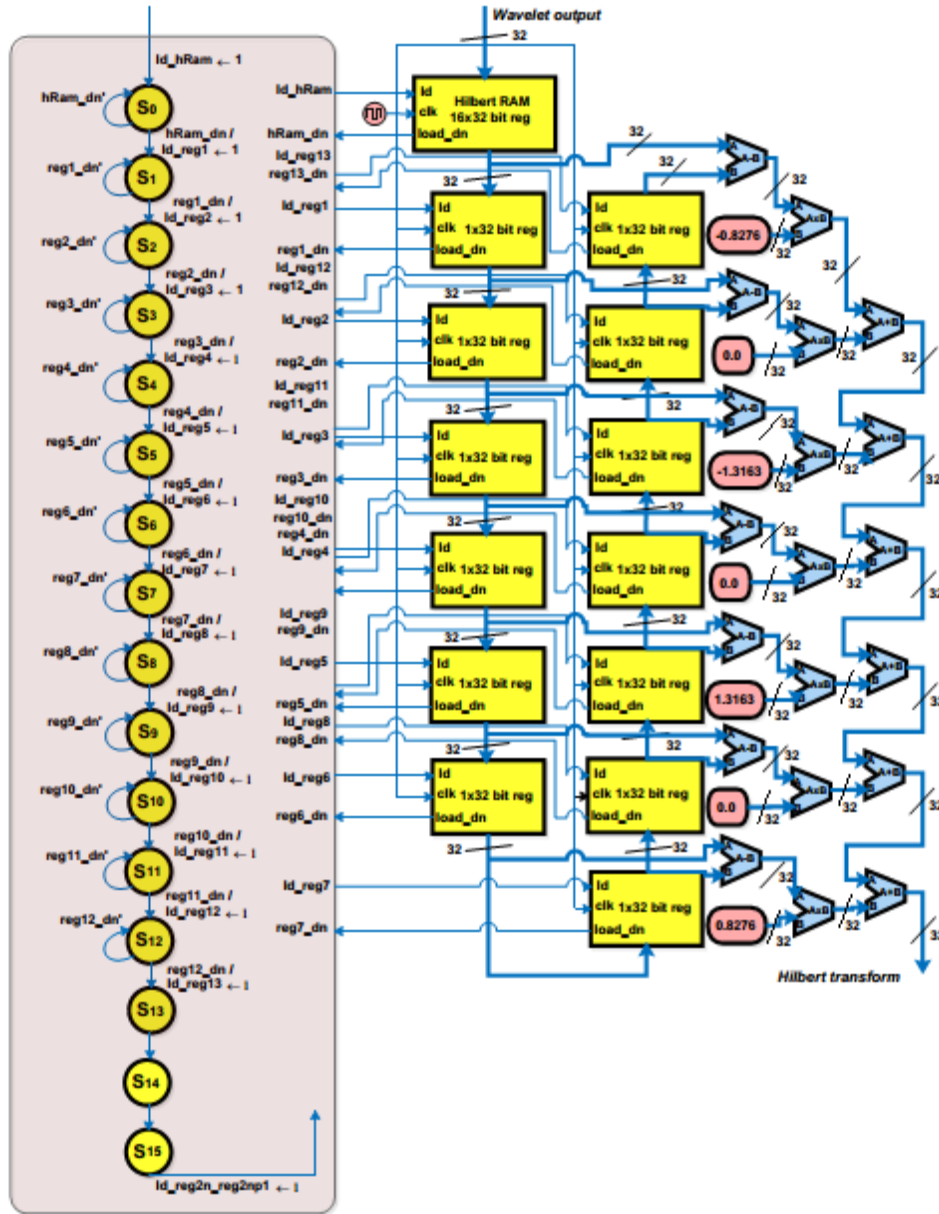


Figure 8. Hilbert processor stage design using CFSM

TABLE VI. COMPARISON BETWEEN PROPOSED FLOATING POINT MULTIPLIER AND XILINX IP CORE FLOATING POINT MULTIPLIER

Operation	Decimal Number	IEEE-754 Floating Point Representation	RMSE
Input 1	1.2915000	00111111101001010100111111011111	
Input 2	9.3453000	01000001000101011000011001011001	
sum - xilinx IP CORE adder	12.0694549	01000001010000010001110001111100	0.000000000
product - proposed adder	12.0694549	01000001010000010001110001111100	
Input 1	-2.3682000	11000000000101111001000010010111	
Input 2	6.4152000	01000000110011010100100101010010	
sum - xilinx IP CORE adder	-15.1924766	11000001011100110001010001100011	0.000000000
product - proposed adder	-15.1924766	11000001011100110001010001100011	



TABLE VII. COMPARISON BETWEEN PROPOSED FLOATING POINT ADDER/SUBTRACTOR AND XILINX IPCORE FLOATING POINT ADDER/SUBTRACTOR

Operation	Decimal Number	IEEE-754 Floating Point Representation	RMSE
sum - xilinx IP CORE adder	Input 1	1.2915000	0011111110100101010011111011111
	Input 2	9.3453000	01000001000101011000011001011001
	sum	10.6368000	01000001001010100011000001010101
	sum - proposed adder	10.6367990	01000001001010100011000001010100
difference - xilinx IP CORE	Input 1	-2.3682000	11000000000101111001000010010111
	Input 2	6.4152000	01000000110011010100100101010010
	difference	4.0470000	01000000100000011000000100000110
	difference - proposed subtractor	4.0470004	01000000100000011000000100000111

To test the performance of the wavelet stage of the processor, the 32x32 bit register was populated with 32 data points each being 32bits wide. Simulation was performed as shown in Fig. 11, where the wavelet stage of the processor can be seen computing the first update and predict values at the rising edge of the clock at 123250ns. The last or sixteenth values of the update and predict values were computed at 124750ns. Fig. 12 shows a zoomed-in view of some values computed by the wavelet processor stage; the values shown are for the first two and sixteenth values of both the update signal and predict signal. To get to these results, the wavelet stage performed all the computations in (6).

Table 8 shows the data points that were used in testing the wavelet stage of the processor, alongside the complete computed update and predict values. To further validate the results obtained in Table 8, a model of the wavelet processor stage was developed using Simulink as shown in Fig. 13, and the results obtained confirm the

accuracy of the wavelet processor stage. The update signal and the predict signal are fed concurrently into two versions of the Hilbert transform that was designed according to the architecture in Fig. 8. Simulation was performed as shown in Fig. 14, where it can be that the first Hilbert transform for the update and predict values were computed at 311550ns, and the last Hilbert transform for the update and predict values were computed at 313050ns. A comparison between Fig. 11 and 14 shows that the Hilbert transform computations started after the completion of the wavelet processor stage computations. This is not unexpected based on the architecture proposed in Fig. 7 and 8. The results obtained from the simulation in Fig. 14 are shown in Table 9, where the Hilbert transform of the update and predict signals are presented. A zoomed-in view of some of the results obtained in Fig. 14 is shown in Fig. 15 for the first two values and the sixteenth value of the update signal and predict signal respectively.

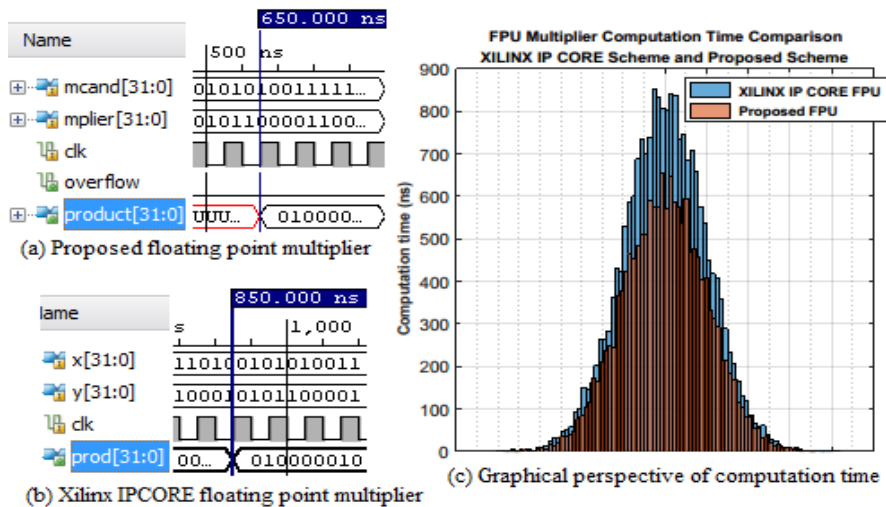


Figure 9. Floating point multiplier product computing time

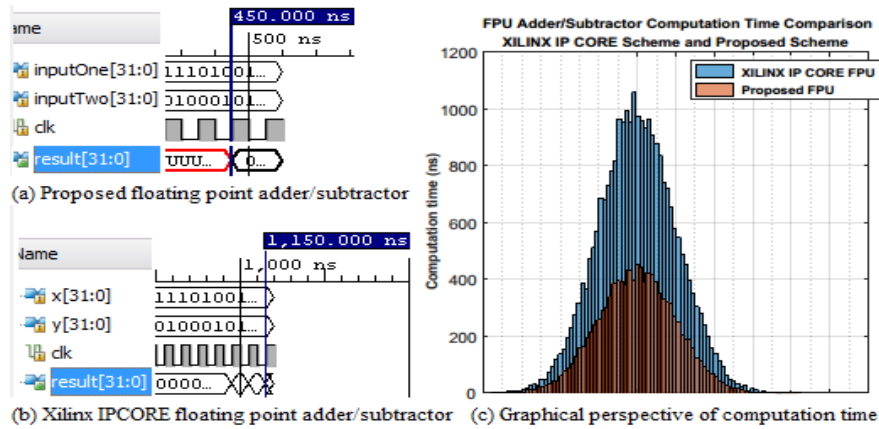


Figure 10. Floating point adder/subtractor computing time

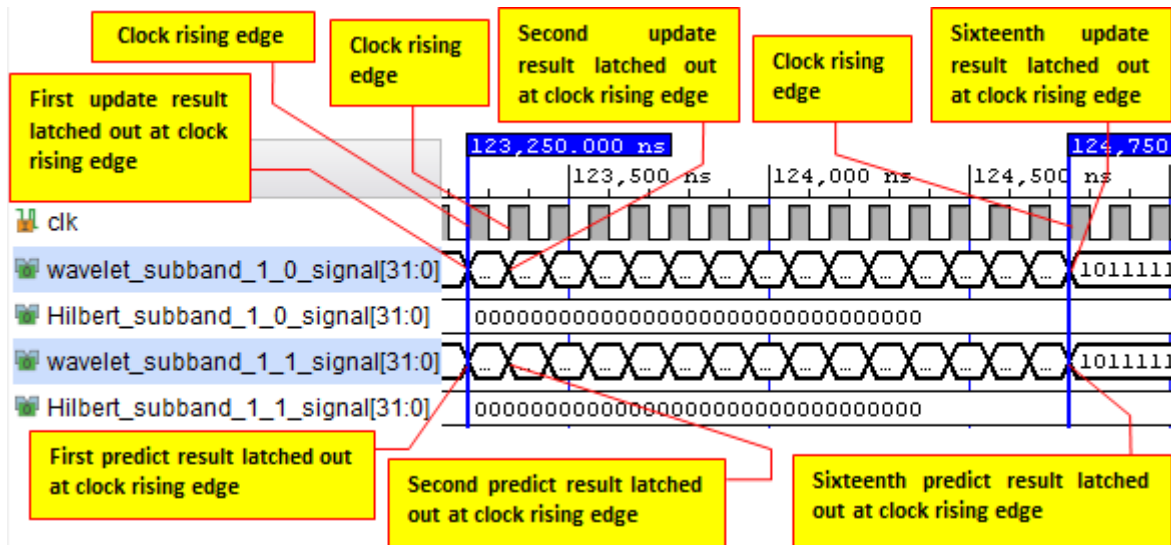


Figure 11. Computation of predict and update values by wavelet stage of processor

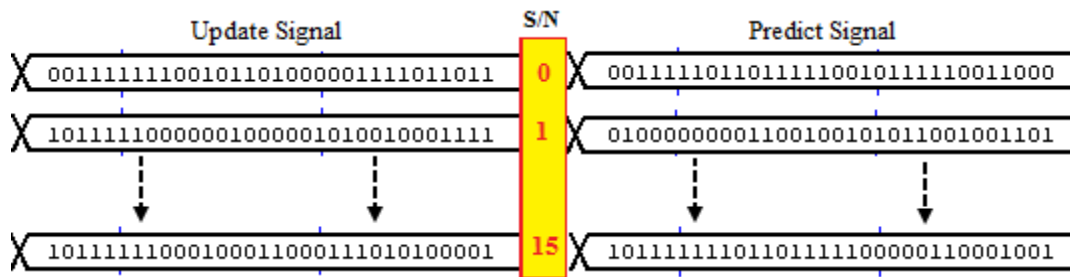


Figure 12. Zoomed-in view of first two and sixteenth wavelet transform values



TABLE VIII. TEST DATA AND COMPUTED RESULTS FOR PROCESSOR WAVELET STAGE

S/N	Input signal value			S/N	IEEE-754 format		Decimal
	IEEE-754 format	Decimal			IEEE-754 format	Decimal	
0	0011111100001001101001101010101	0.5377	Update signal	0	00111111100101101000001111011011	1.175898	
1	00111111111010101011110100111100	1.8339		1	10111110000001000001010010001111	-0.12898	
2	11000000000100001001000000101110	-2.2588		2	1011111100010100110110100111011	-1.08145	
3	00111111010111001011100100100100	0.8622		3	00111111000001010101011001000001	0.52084	
4	00111110101000110011100111000001	0.3188		4	0100000001010100101111011010010	3.34953	
5	1011111101001110110001010110111	-1.3077		5	01000000000000111010111010011001	2.05753	
6	1011111011011110000000011010010	-0.4336		6	00111110111101111111001100000110	0.48427	
7	00111110101011110110100101000100	0.3426		7	1011110101000000010011000111011	-0.04691	
8	01000000011001010000010010000001	3.5784		8	00111111101010001100100010101110	1.31862	
9	0100000001100010011110111011001	2.7694		9	0100000000010110000111010001000	2.17276	
10	1011111101011001100100110000110	-1.3499		10	10111111001111000110100111011011	-0.73598	
11	01000000010000100011101111001101	3.0349		11	0011111110101111100011000110110	1.68573	
12	00111111001110011011001111010000	0.7254		12	00111111101001101110010001011111	1.30384	
13	10111101100000010011101010010011	-0.0631		13	00111110100001111011000101010100	0.26502	
14	00111111001101101111011010010100	0.7147		14	10111110001011010010000011011010	-0.16907	
15	10111110010100011110101110000101	-0.2050	15	10111111000100011000111010100001	-0.56858		
16	1011101111111100010100000100100	-0.1241	Predict signal	0	00111110110111110010111110011000	0.43591	
17	0011111101111101010111001111101	1.4897		1	01000000001100100101011001001101	2.78651	
18	0011111101101000101101000011101	1.4090		2	1011111101111110100111101101001	-0.99730	
19	001111110110101010011011001111	1.4172		3	0011111010001101011111010111101	0.27634	
20	0011111100101011110011101101101	0.6715		4	1011111110100010100110010001100	-1.63514	
21	101111110010101000111101011100	-1.2075		5	0100000001101010101011110001100	3.67868	
22	00111111001101111001101001101011	0.7172		6	10111110000001101110111100101111	-0.13177	
23	0011111110100001010101001100101	1.6302		7	1011111100011101111110100000111	-0.61714	
24	00111110111110100101000100011010	0.4889		8	0011111101011110101010100101001	0.86982	
25	00111111100001000111000100001101	1.0347		9	10111110001101001001100001011101	-0.17636	
26	00111111001110100001011000011110	0.7269		10	10111111001001010001110010000111	-0.64496	
27	1011111010011010101011100111111	-0.3034		11	00111011011011111111100101011000	0.00366	
28	00111110100101100111101000010000	0.2939		12	00111111000011001000011000111101	0.54892	
29	10111111010010011000110001111110	-0.7873		13	1011111011101010011101100110011	-0.45943	
30	00111111011000110110111000101111	0.8884		14	10111111000110011001101111101000	-0.60003	
31	1011111100100101101010000101100	-1.1471	15	1011111101101111100000110001001	-1.43559		

A verification model based on the Hilbert FIR structure in Fig. 8 was developed and tested as shown in Fig. 16. A comparison between the results shown in Table 10 and Fig. 16 confirms the accuracy of the Hilbert transform processor stage.

A second comparison in the context of FPGA resource utilization was also made between the design of the Hilbert transform processor presented in this paper and similar other designs; this is shown in Table 10 where it can be seen the Hilbert processor in this paper performs well in comparison with similar designs.

**8. CONCLUSION**

In this paper, we undertook the design of a processor that computed the DWPT and then the Hilbert transform of the DWPT of an input signal. The design approach was based on the lifting steps of a Db4 wavelet for the DWPT, and FIR technique for the Hilbert transform. Using these approaches, an architecture was developed for the processor datapath, after which the processor unit was also developed. The arithmetic and logic unit (ALU) of the datapath in Figs 7 and 8 were designed to perform three basic primitive arithmetic operations:

multiplication, addition, and subtraction. These operations are floating point in nature based on the IEEE-754 single precision floating point arithmetic owing to the fact that the data representation in the VLSI design of the processor is also based on the IEEE-754 single precision floating point format. Simulation results were used to verify the performance of the processor, where the DWPT of the input signal was computed based on the lifting steps, and then the Hilbert transform of the DWPT signal was subsequently computed in the second stage of the processor. The waveform analysis of the results and the tabulation of the simulation results confirmed that the processor performed as expected.

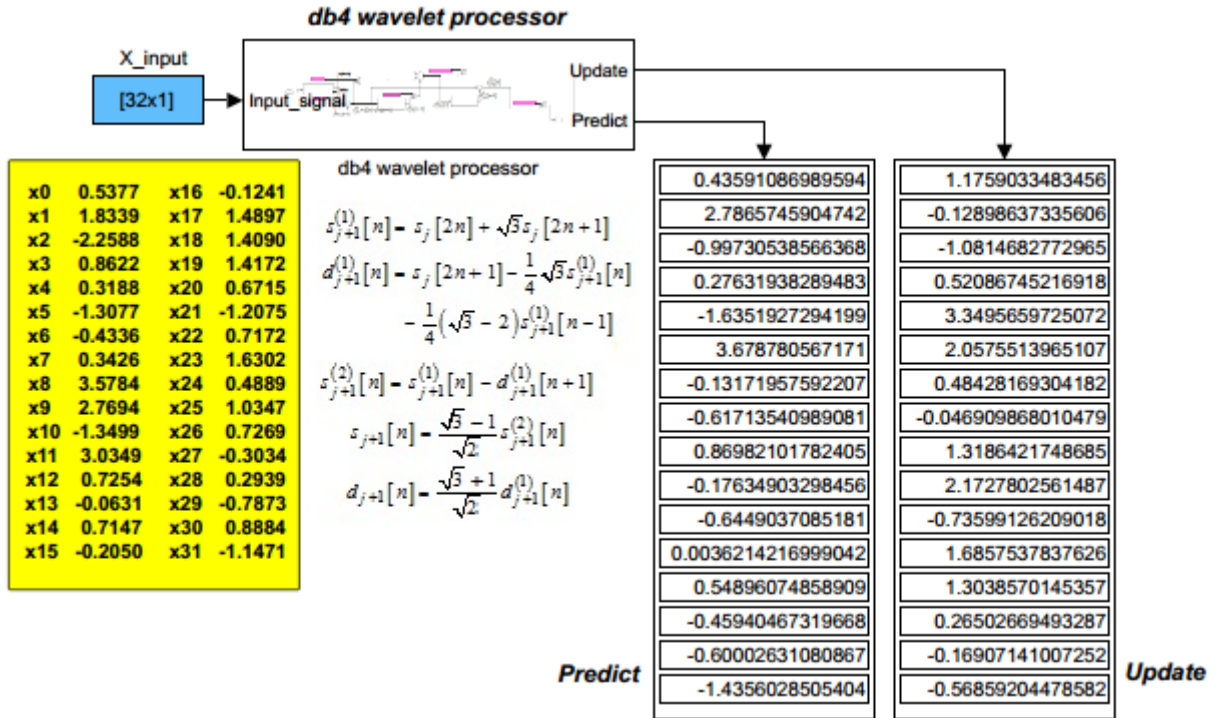


Figure 13. Simulink verification model for wavelet processor stage

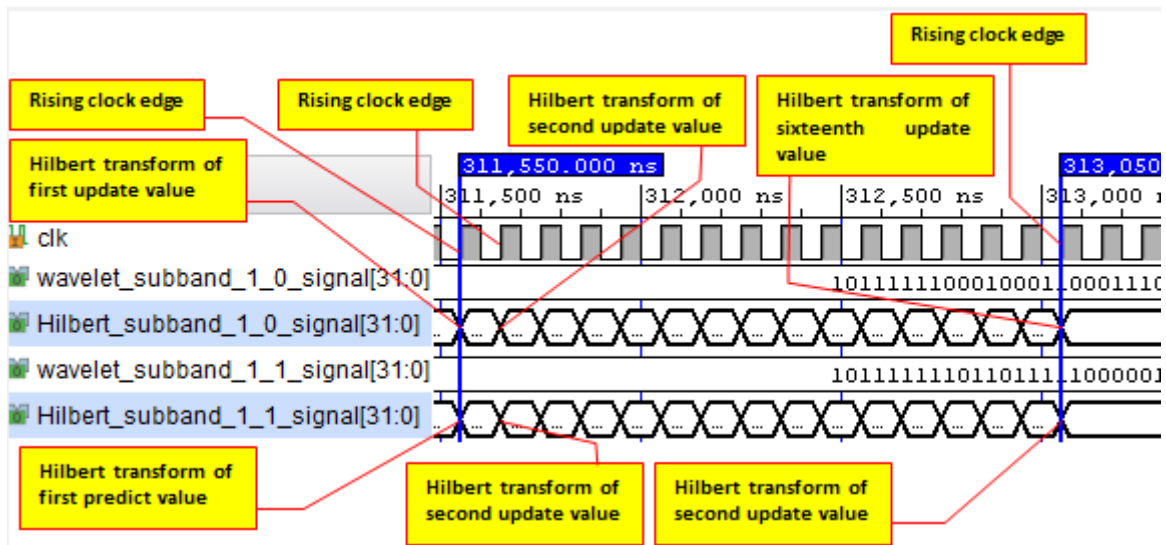


Figure 14. Computation of the Hilbert transform of update and predict values



TABLE IX. HILBERT TRANSFORM OF UPDATE AND PREDICT SIGNALS

S/N	IEEE-754 format	Decimal	IEEE-754 format	Decimal	
Update signal	0	00111111100101101000001111011011	1.17589	10111111011110010010000111101101	-0.97317
	1	1011111000001000001010010001111	-0.12898	00111101110110101001111010001100	0.10674
	2	1011111100010100110110100111011	-1.08145	10111111001001110001111101000010	-0.65282
	3	0011111100001010101011001000001	0.52084	10111110100001011100010101001000	-0.26127
	4	01000000010101100101111011010010	3.34953	00111110010011000001000010101000	0.19928
	5	01000000000000111010111010011001	2.05753	11000000001000111011100101010101	-2.55818
	6	0011111011110111111001100000110	0.48427	11000000101010000101001100000001	-5.26013
	7	1011110101000000010011000111011	-0.04691	11000000010001000001010111011111	-3.06383
	8	00111111101010001100100010101110	1.31862	0011111111100100010110010000010	1.89198
	9	0100000000010110000111010001000	2.17276	0011111101000000000100010111000	0.75013
	10	10111111001111000110100111011011	-0.73598	01000000000000010110001011011100	2.02164
	11	0011111110101111100011000110110	1.68573	11000000000110101000101110110000	-2.41476
	12	00111111101001101110010001011111	1.30384	10111111000010000010111101011100	-0.53198
	13	001111110100001111011000101010100	0.26502	11000000100111000001001000101110	-4.87720
	14	10111110001011010010000011011010	-0.16907	11000000011000101101100010111111	-3.54446
	15	10111111000100011000111010100001	-0.56858	01000000101111011001000111011011	5.92405
Predict signal	0	001111101101111110010111110011000	0.43591	10111110101110001011010101101010	-0.36075
	1	01000000001100100101011001001101	2.78651	11000000000100111001011101111111	-2.30612
	2	10111111011111110100111101101001	-0.99730	00111110100000001100111101010000	0.25158
	3	00111110100011010111110101111101	0.27634	11000000011110010110000111011101	-3.89659
	4	1011111110100010100110010001100	-1.63514	0100000010011110101100010111001	3.23979
	5	01000000011010110110111110001100	3.67868	00111110100001001111000111011000	0.25965
	6	10111110000011011101111001011111	-0.13177	0011111101001111001101010011110	1.30940
	7	10111111000111011111110100000111	-0.61714	11000000000000010110111011000010	-2.02238
	8	0011111101011101010110100101001	0.86982	11000000101110101001000101110111	-5.83025
	9	10111110001101001001100001011101	-0.17636	01000000110010001111110010100010	6.28083
	10	1011111001001010001110010000111	-0.64496	11000000110000010001101001110110	-6.03448
	11	0011011011011111111100101011000	0.00366	01000000101101100110111011101010	5.70103
	12	00111111000011001000011000111101	0.54892	0011111110110000101100111010100	1.69024
	13	10111110111010110011101100110011	-0.45943	00111111011100010010000111011100	0.94192
	14	10111111000110011001101111101000	-0.60003	110000000000000100010001010100	-2.01668
	15	10111111011011111100000110001001	-1.43559	1011111111011111010101101111011	-1.87242

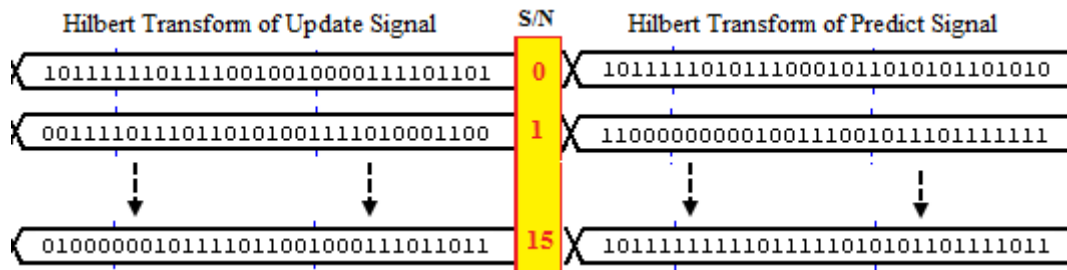


Figure 15. Zoomed-in view of first two and sixteenth values of Hilbert transform

TABLE X. PERFORMANCE COMPARISON OF PROPOSED HILBERT TRANSFORM PROCESSOR WITH SIMILAR PROCESSORS

Title of work	LUTs	FF	IoBs	BRAM	Mults	DSP	GCLK	BUF
FPGA-Based implementation of instantaneous frequency estimation of Embedded Hilbert transform based algorithm within an FPGA to classify	5,555	2,168	49	2	4	-	1	-
Efficient Architecture For Real Time Implementation of Hilbert Transform in	8,511	7,078	-	26	20	-	-	-
A High Performance Pipelined Discrete Hilbert Transform Processor [40]	3,525	2,168	49	-	-	-	-	-
Ultrasound B-Mode Back End Signal Processor on FPGA [41]	6,486	5,268	-	-	-	-	-	-
<b>Proposed Hilbert Transform processor</b>	<b>2,597</b>	<b>4,536</b>	<b>34</b>	<b>-</b>	<b>-</b>	<b>2</b>	<b>-</b>	<b>1</b>

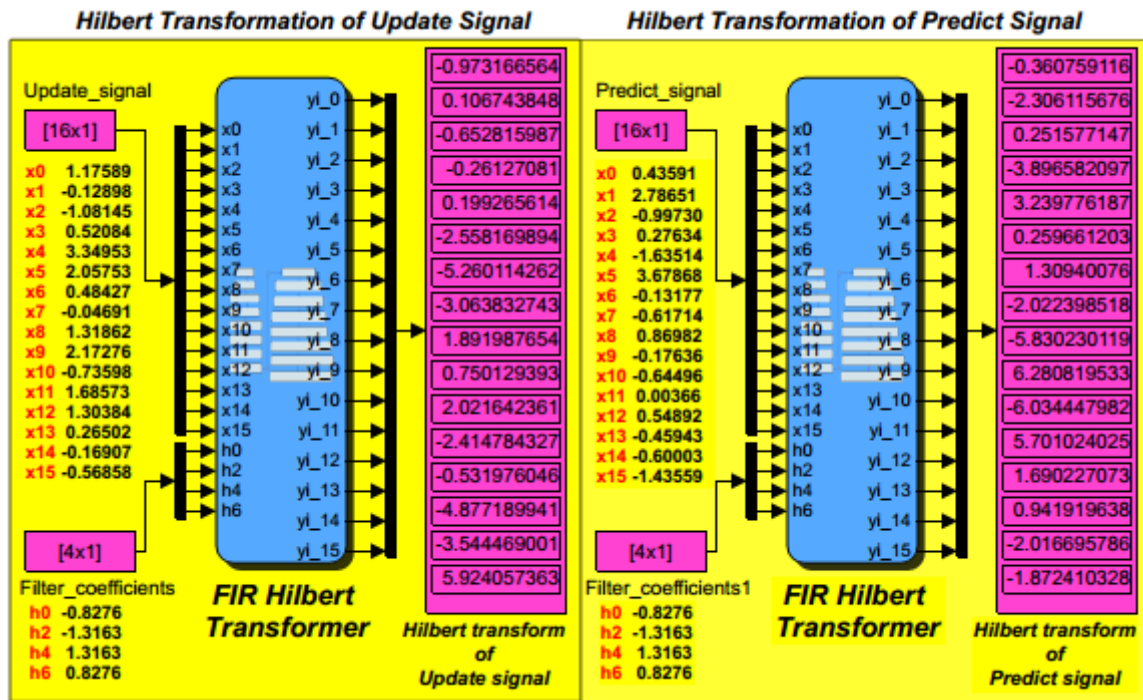


Figure 16. Simulink-State flow verification model for Hilbert transform

## REFERENCES

- [1] P. Y. Dibal, E. N. Onwuka, J. Agajo, and C. Alenoghena, "Enhanced Discrete Wavelet Packet Sub-band Frequency Edge Detection using Hilbert Transform," *Int. J. Wavelets, Multiresolution Inf. Process.*, vol. 16, no. 1, pp. 1850009-1-1850009-17, 2018.
- [2] H. Wang and X. Chen, "Development and Optimization Design of Digital Logic device based on FPGA," *J. Phys. Conf. Ser.*, vol. 1345, no. 062051, pp. 1-9, 2019.
- [3] J. Ashenden, P. *Digital Design: An Embedded Systems Approach using VHDL*. Burlington: Morgan Kaufmann.
- [4] P. Chu, P. *FPGA Prototyping by VHDL Examples*. New Jersey: John Wiley & Sons, 2008.
- [5] M. Ravi, A. Sewa, S. T.G., and S. S. S. Sanagapati, "FPGA as a Hardware Accelerator for Computation Intensive Maximum Likelihood Expectation Maximization Medical Image Reconstruction Algorithm," *IEEE Access*, vol. 7, pp. 111727-111735, 2019.
- [6] R. Krishnamoorthy, P. T. Kalaivaani, and A. S. Reddy, "An Advanced Multiplier less Prediction Scheme based on Discrete Wavelet Transformation Approach for Image Analysis," *Int. J. Recent Technol. Eng.*, vol. 7, no. 4S, pp. 511-518, 2018.
- [7] H. I. Shahadi, R. Jidin, and H. Way, W. "High Performance FPGA Architecture for Dual Mode Processor of Integer Haar Lifting-Based Wavelet Transform," *Int. Rev. Comput. Softw.*, vol. 8, no. 9, pp. 2058-2067, 2013.
- [8] M. A. FARAHANI and M. ESHGHI, "Implementing a New Architecture of Wavelet Packet Transform on FPGA," in *8th WSEAS International Conference on Acoustics & Music: Theory & Applications*, 2007, pp. 37-41.
- [9] Y. Liu and E. K. Lai, "Design and Implementation of An RNS-Based 2-D DWT Processor," *IEEE Trans. Consum. Electron.*, vol. 50, no. 1, pp. 376-386, 2004.
- [10] W. Xu, Z. YAN, and D. SHUNYING, "A High Performance Pipelined Discrete Hilbert Transform Processor," *WSEAS Trans. Signal Process.*, vol. 1, no. 9, pp. 21-30, 2013.
- [11] A. A. Assef, B. M. Ferreira, J. M. Maia, and E. T. Costa, "Modeling and FPGA-based implementation of an efficient and simple envelope detector using a Hilbert Transform FIR filter for ultrasound imaging applications," *Research Biomed. Eng.*, vol. 34, no. 1, pp. 87-92, 2018.
- [12] H. Nikookar, *Wavelet Radio: Adaptive and Reconfigurable Wireless Systems Based on Wavelets*. Cambridge: Cambridge University Press, 2013.
- [13] Y. Arjoune and N. Kaabouch, "A Comprehensive Survey on Spectrum Sensing in Cognitive Radio Networks: Recent Advances, New Challenges, and Future Research Directions," *MDPI Sensors*, vol. 19, no. 126, pp. 1-32, 2019.
- [14] Q. Zhinjin, N. Wang, G. Yue, and C. Laurie, "Adaptive Threshold for Energy Detector Based on Discrete Wavelet Packet Transform," in *Wireless Telecommunications Symposium*, 2012, pp. 1-5.
- [15] N. Wei, Z. Chen, and A. Zhu, "Research on Adaptive Resolution Spectrum Sensing Method Based on Discrete Wavelet Packet Transform," *Telkommika Indones. J. Electr. Eng.*, vol. 12, no. 2, pp. 1385 - 1394, 2014.
- [16] I. Daubechies and W. Sweldens, "Factoring Wavelet Transforms into Lifting Steps," *J. Fourier Anal. App.*, vol. 4, pp. 247 - 269, 1998.
- [17] W. Lewis, D. *Fundamentals of Embedded Software: Where C and Assembly meet*. New Jersey: Prentice Hall, 2002.



- [18] K. Mishra, S. V. Nandanwar, A. Ayele, E. and B. Dhok, S, "FPGA Implementation of Single Precision Floating Point Multiplier using High Speed Compressors," *Int. J. Soft Comput. Eng.*, vol. 14, no. 2, pp. 18–23, 2014.
- [19] R. Fay, A. Hsieh, D. Jeang, and B. Jenkins, "A Synthesizable VHDL Floating Point Package." John Hopkins University ECE Department, 2011.
- [20] U. Concordia, "Concordia, University Lectures," 2010. [Online]. Available: [http://users.encs.concordia.ca/~asim/COEN\\_6501/Lecture\\_Notes/L4\\_Slides.pdf](http://users.encs.concordia.ca/~asim/COEN_6501/Lecture_Notes/L4_Slides.pdf). [Accessed: 11-Jun-2018].
- [21] Z. Peng, P. Tse, and F. Chu, "A comparison study of improved Hilbert-Huang transform and wavelet transform: Application to fault diagnosis for rolling bearing," *Mech. Syst. Signal Process.*, vol. 19, pp. 974 – 988, 2005.
- [22] N. Saravanan, "Gear box Fault Diagnosis using Hilbert Transform Feature Classification by PVSM," *Int. J. Adv. Res. Comput. Sci. Softw. Eng.*, vol. 6, no. 6, pp. 21 – 30, 2016.
- [23] A. Fedotov, A. Akulova, and S. Akulov, "Effective QRS-Detector Based on Hilbert Transform and Adaptive Thresholding," in *XIV Mediterranean Conference on Medical and Biological Engineering and Computing*, 2016, pp. 140 – 144.
- [24] S. Aditi, "Survey Paper on Hilbert Transform with its Application in Signal Processing," *Int. J. Comput. Sci. Inf. Technol.*, vol. 5, no. 3, pp. 3880 – 3882, 2014.
- [25] E. Romero, D. G. Jimenez, M. and G. Dolecek, J, "On the Estimation of Minimum Number of Distinct Multipliers in FIR Hilbert Transformers Based on Frequency Transformation," in *The 2013 Iberoamerican Conference on Electronics Engineering and Computer Science*, 2013, pp. 88–95.
- [26] G. Lyons, R, *Understanding Digital Signal Processing*, 2nd ed. New Jersey: Prentice Hall, 2004.
- [27] S. Diniz, P, A. Silva, E, and L. Netto, S, *Digital Signal Processing: System Analysis and Design*, 2nd ed. New York: Cambridge University Press, 2010.
- [28] J. Orfanidis, S, *Introduction to Signal Processing*. New York: Prentice Hall, 2010.
- [29] K. Ingle, V and G. Proakis, J, *Digital Signal Processing using MATLAB*, 3rd ed. Stamford CT: Cengage Learning, 2010.
- [30] F. Harris, J, "On the Use of Windows for Harmonic Analysis with Discrete Fourier Transform," *Proc. IEEE*, no. 1, pp. 51–83, 1978.
- [31] S. Chakraborty, "Advantages of Blackman Window over Hamming Window Method for Design of FIR Filter," *Int. J. Comput. Sci. Eng. Technol.*, vol. 4, no. 8, pp. 1181–1189, 2013.
- [32] Xilinx, "Xilinx FIR Compiler v7.2," 2020. [Online]. Available: [https://www.xilinx.com/support/documentation/ip\\_documentation/fir\\_compiler/v7\\_2/pg149-fir-compiler.pdf](https://www.xilinx.com/support/documentation/ip_documentation/fir_compiler/v7_2/pg149-fir-compiler.pdf). [Accessed: 17-May-2020].
- [33] A. Benso, "Introduction to Complex FSMs Design." Torino, pp. 1–38, 2011.
- [34] A. A. Prince, P. K. Verma, C. Jayakumar, and D. Raju, "Efficient Architecture For Real Time Implementation of Hilbert Transform in FPGA," in *Electrical, Computer and Communication Technologies (ICECCT), 2015 IEEE International Conference on. IEEE*, 2015, pp. 1–5.
- [35] M. D. Linderman, M. Ho, D. L. Dill, T. H. Meng, and G. P. Nolan, "Towards Program Optimization through Automated Analysis of Numerical Precision," in *Proc CGO*, 2010, pp. 230–237.
- [36] T. Aamodt and P. Chow, "Numerical error minimizing floating-point to fixed-point ANSI C compilation," in *1st Workshop on Media Processors and DSPs*, 1999, pp. 3–12.
- [37] N. Wiebe and V. Kliuchnikov, "Floating point representations in quantum circuit synthesis," *New J. Phys.*, vol. 15, no. 093041, pp. 1–25, 2013.
- [38] E. Hernandez, J. Toledo, J. Martinez, and R. Ruiz, "FPGA-based implementation of the instantaneous frequency estimation of phonocardiographic signals," in *International Federation of Auto. Control workshop on Programmable Devices and Systems*, 2004, pp. 423–428.
- [39] J. D. Jones, J. S. Pei, and M. P. Tull, "Embedded Hilbert transform based algorithm within an FPGA to classify nonlinear SDOG systems," in *Proceedings of the 23rd International Modal Analysis Conference*, 2008.
- [40] W. Xu, Z. Yan, and D. Shunying, "A High Performance Pipelined Discrete Hilbert Transform Processor," *WSEAS Trans. SIGNAL Process.*, vol. 9, no. 1, pp. 1–6, 2013.
- [41] U. k Jayaraj, S. Gayathri, and A. Shamy, "Ultrasound B-Mode Back End Signal Processor on FPGA," *Int. J. Eng. Res. Technol.*, vol. 4, no. 6, pp. 583–588, 2015.



**Peter Yusuf Dibal** has a PhD student in communication at the Federal University of Technology Minna. He holds a Master's degree in Electronics and Communications Engineering from Teesside University in the UK. His research interests are digital signal processing, communications, and VLSI design.



**Elizabeth N. Onwuka** is a Professor of Telecommunications Engineering. She holds a PhD in Communications and Information Systems Engineering, from Tsinghua University, Beijing, People's Republic of China; a Master of Engineering degree, in

Telecommunications; and a Bachelor of Engineering degree from Electrical and Computer Engineering Department, Federal University of Technology (FUT) Minna, Niger State, Nigeria. Her research interest includes Mobile communications network, Mobile IP networks, Handoff management, Paging, Network integration, Resource management in wireless networks, spectrum management, and Big Data Analytics.



**James Agajo** has a PhD in the field of Telecommunication and Computer, Signal Processing. He also has a Master's Degree in Electronic and Telecommunication Engineering. His research interest is in Wireless Sensor Systems, and Network and intelligent system development.



**Caroline O. Alenoghena** holds a PhD in Telecommunications Engineering, and a Master's degree in Electronics Telecommunications. She is a member of the Institute of Electrical and Electronic Engineers MIEEE, Nigerian Society of Engineers (NSE), and Association of Professional Women Engineers of Nigeria APWEN. She is a registered practicing Engineer with the Council for the Regulation of

Engineering in Nigeria. Her research interests include intelligent systems and networks.



**Achonu Adejo** obtained a first degree in Electrical/Computer Engineering from Federal University of Technology Minna, Nigeria in 2006, an MSc in Electronic Communications and Computer Engineering from University of Nottingham (Malaysia campus) in 2010 and a PhD in Electrical Engineering from

Newcastle University, UK in 2018. His doctorate program was carried out in the Communications, Sensors and Signal processing group at School of Engineering. Since 2010, he has been an academic staff with Federal University of Technology Minna. His research interests and previous works are in Minimal computer processors, FPGAs, Resource management and modelling of Cellular communications with focus on 5G communications and D2D networks.